PRAMANA — journal of physics

Vol. 82, No. 2
February 2014
pp. 313–319

A comparative study on dual colour soft aperture cascaded second-order mode-locking with different nonlinear optical crystals

SHYAMAL MONDAL[1], SATYA PRATAP SINGH[1], SOURABH MUKHOPADHYAY[2], ADITYA DATE[1], KAMAL HUSSAIN[1], SHOUVIK MUKHERJEE[1] and PRASANTA KUMAR DATTA[1,*]

[1]Department of Physics, Indian Institute of Technology Kharagpur, Kharagpur 721 302, India
[2]Department of Physics, Jhargram Raj College, Jhargram 721 507, India
*Corresponding author. E-mail: pkdatta.iitkgp@gmail.com

DOI: 10.1007/s12043-014-0683-z; ***e*Publication:** 9 February 2014

Abstract. A comparative study in terms of optimized output power and stability is made on cascaded second-order nonlinear optical mode-locking with KTP, BBO and LBO crystals for both 1064 nm and 532 nm. Large nonlinear optical phase shift achieved in a non-phase-matched second harmonic generating crystal, is transformed into amplitude modulation through soft aperturing the nonlinear cavity mode variation at the laser gain medium to mode-lock a Nd:YVO_4 laser. The laser delivers stable dual wavelength cw mode-locked pulse train with pulse duration 10.3 ps and average power of 1.84 W and 255 mW at 1064 nm and 532 nm respectively for the optimum performance in type-II KTP crystal. The exceptional stability achieved with KTP is accounted by simulating the mode-size variation with phase mismatch.

Keywords. Mode-locking; ultrafast processes; optical susceptibility; frequency conversion; dynamics of nonlinear optical systems.

PACS Nos 42.60.Fc; 42.65.Re; 42.65.An; 42.65.Ky; 42.65.Sf

1. Introduction

Kerr-lens mode-locking (KLM), which uses self-focussing effect in gain medium due to intrinsic third-order nonlinearity $\chi^{(3)}$ of the medium, has been found to be very efficient and reliable in femtosecond (fs) regime [1,2]. However, in picosecond (ps) regime, KLM is not effective since the low intracavity peak power cannot generate the required nonlinear loss modulation due to weak intrinsic $\chi^{(3)}$ of the medium. However, in a second-order cascaded process, where two second-order nonlinear optical interactions occur simultaneously in a nonlinear crystal, a large effective third-order nonlinearity ($\chi^{(3)}_{\text{eff}}$) can

be produced that can mimic the effects of third-order nonlinear optical processes in a second-order nonlinear optical crystal at a much lower power [3,4].

This cascaded process can also be applied for mode-locking, namely second-order nonlinear optical mode-locking (CSM) [5–7], a SHG crystal is placed in off-phase-matched condition and uses the real part of the induced ($\chi_{\text{eff}}^{(3)}$). It does not provide direct amplitude modulation as in nonlinear mirror mode-locking (NLM) [8,9], rather forward and return pass through the nonlinear crystal (NLC) imprints a nonlinear phase shift (Φ_{NL}) on the FW beam giving nonlinear mode size variation, which in turn can be converted into nonlinear loss modulation with a suitably placed aperture inside the laser cavity. The scheme is analogous to that of KLM but effective in ps regime as it uses large induced ($\chi_{\text{eff}}^{(3)}$) originating from cascaded second-order nonlinearity. However, the placement of the aperture is critical since it has to be placed accurately at the intracavity position where mode-size variation is the maximum.

To the best of our knowledge, in the present work, soft aperture dual wavelength CSM in various crystals is investigated for the first time and the performance is compared in terms of stability and output power. In the absence of any physical aperture, nonlinear loss modulation is achieved due to cavity mode size reduction with increase in intracavity power at the gain medium. Thus, effective gain increases due to better overlapping between pump and the cavity mode. A comparative study of cascaded second-order mode-locking (CSM) with different choices of nonlinear crystal as well as the output coupler (OC), is made to optimize the performance. In the optimum case, stable mode-locked pulse train of ∼10 ps width and maximum output power of 1.84 W and 255 mW at 1064 nm and 532 nm respectively are generated simultaneously in type-II potassium titanyl phosphate ($KTiOPO_4$) (KTP) from a single laser oscillator for a pump power of 12 W.

2. Experiment

The schematic diagram of the laser lay-out is shown in figure 1. The pump is a 808 nm fibre-coupled laser diode array of 12 W maximum output power and is focussed to a spot size of 240 μm at the centre of the gain medium which is a $4 \times 4 \times 8$ mm^3, a-cut, Nd:YVO_4 crystal having Nd^{3+} concentration of 0.5%. The rear face of the RM is antireflection-coated at 808 nm and has high reflectivity (>99.5%) at 1064 nm on the other side. The Nd:YVO_4 crystal is antireflection-coated on both its parallel faces for 1064 nm and 808 nm wavelengths and is tilted by an angle of 2° to reduce the effect of

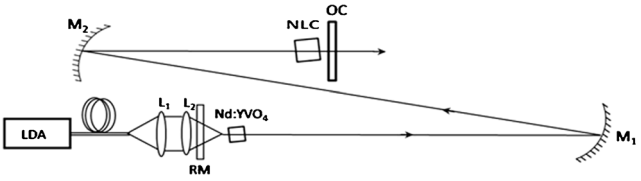

Figure 1. Schematic of the soft aperture CSM laser. LDA: laser diode array, L_1 and L_2: focussing lenses, RM: rear mirror, M_1 and M_2: folding mirrors, OC: output coupler.

undesired reflections inside the cavity. Two concave mirrors M_1 and M_2 of 500 mm and 250 mm radius of curvature respectively are used to focus the beam at the OC. The tilting angle of M_1 and M_2 is kept as low as possible to avoid cavity astigmatism, thus providing TEM_{00} mode throughout the cavity which has been found to be necessary for stable cw ML operation. A second harmonic crystal, usually in non-phase-matched condition, is placed near the OC. Different nonlinear crystals, such as KTP (positive biaxial crystal, cut for type-II SHG of 1.064 μm: $\theta = 90°$, $\varphi = 23.5°$, size: $7 \times 7 \times 9$ mm^3), BBO (negative uniaxial crystal, cut for type-I SHG of 1.064 μm: $\theta = 22.8°$, $\varphi = 90°$, size: $6 \times 6 \times 12$ mm^3) and LBO (negative uniaxial crystal, cut for type-I SHG of 1.064 μm: $\theta = 90°$, $\varphi = 11.3°$, size: $5 \times 5 \times 15$ mm^3) are used in combination with different OC, to optimize the laser performance with respect to the pulse width and output power. The different arms of the Z-shaped passive cavity of 81.7 cm length are optimized to be 250 mm, 405 mm and 162 mm respectively which gives a cavity mode size of around 213−280 μm at the gain medium for different crystals. Stable mode-locked operation is obtained by tuning the SHG crystal away from the phase-matched condition and then varying the separation between SHG crystal and the OC.

3. Results

Mode-locking is found to be self-starting for all the crystals when it is detuned form phase matching. The variations of output mode-locked power with respect to the input pump power for different crystal and OC combinations are shown in figure 2. The ML sets in for an input pump power of 9 W with KTP and the maximum mode-locked output power achieved are 1.84 W and 255 mW at 1064 nm and 532 nm respectively corresponding to the input pump power of 12 W. Figures 2a, 2b and 2c show the output power for different output couplers available in the laboratory. Figure 2a is for output coupler highly reflective at 1064 nm and 10% reflective at 532 nm (OC-1), 2b is for output coupler of 94% reflective at 1064 nm and 93% reflective at 532 nm (OC-2) and 2c is for output coupler of 92% reflective at 1064 nm and 13% reflective at 532 nm (OC-3). We have seen experimentally that OC-3 with KTP crystal gives the best result compared to others. Owing to the high effective nonlinear coefficient of KTP (3.5 pm/V) and the intracavity effect with OC-3, the laser generates mode-locked pulse train simultaneously at both 1064 nm and 532 nm with output powers of 1.84 W and 255 mW respectively and pulse repetition rate of 178 MHz, which proves the laser to be an efficient dual wavelength ps source. Moreover, the output power can be scaled up since the ML scheme is not restricted by the input pump power. The ML regime is found to be highly stable in both short and long time-scales and is never affected by the Q-switching instability. We have obtained stable mode-locked pulse train with the output power fluctuation below 1% which does not drop even after running for hours. The pulse amplitude fluctuation as measured in oscilloscope is less than 5% of its rms value. The cavity mode size of 442 μm at the gain medium and 213 μm at the centre of the KTP crystal are determined by the ABCD matrix formalism. No mode-locking is observed when the NLC is set at exact phase-matched condition corresponding to $\Delta kL = (k^e_{2\omega} - k^o_{\omega} - k^e_{\omega})L = 0$, where k_i are the wave numbers and L is the length of the NLC. As the crystal is detuned from phase matching by an angle more than $\sim 1°$ in the direction of increasing φ, mode-locking is found to set in, but initially

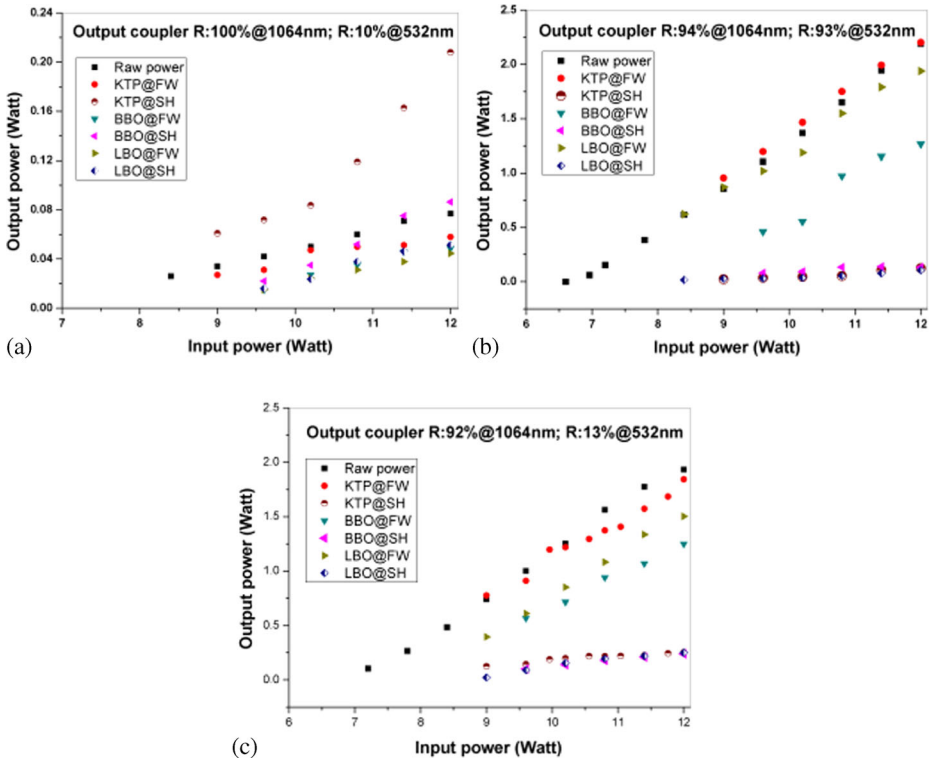

Figure 2. Stable mode-locked output power with input pump power for different output couplers: (**a**) HR@1064 nm and *R*: 10% @ 532 nm, (**b**) *R*: 94% @1064 nm and *R*: 93% @ 532 nm, (**c**) *R*: 92% @1064 nm and *R*: 13% @ 532 nm, FW: 1064 nm, SH: 532 nm.

with a smaller depth of modulation of the mode-locked pulses. Depth of modulation of the mode-locked pulses is found to increase as the phase mismatch angle ($\Delta\varphi$) is continued to increase in the same direction and full depth of modulation is achieved around $\Delta\varphi \approx 1.5°$ for the optimum case. This observation clearly identifies the mechanism of CSM responsible for ML. As the crystal is further detuned, the depth of modulation decreases and when the phase mismatch angle increases above 2°, mode-locking finally disappears. However, no mode-locking is observed for any phase mismatch in the other side of the phase-matching angle. Most stable operation with full depth of modulation of the mode-locked pulses is found to occur when the KTP crystal is set approximately by an angle (φ) of 25°20′. Finally the laser is optimized for stable mode-locked operation by varying the separation between NLC and the OC. For OC-3 and KTP, the optimum case, we show a typical measured trace of non-collinear background-free intensity autocorrelation, employing a 3 mm long BBO crystal, for 1064 nm pulse in figure 3. The FWHM of the autocorrelation trace is measured to be 15.9 ps, corresponding to a pulse width of 10.3 ps for assumed sech^2 pulse shape.

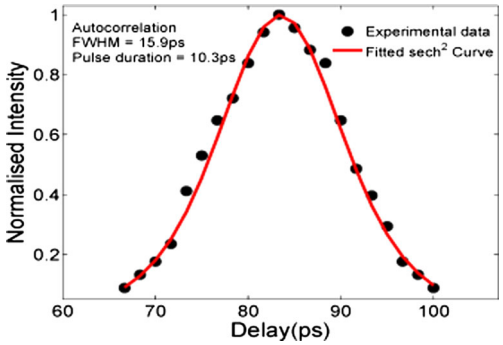

Figure 3. Non-collinear SHG intensity autocorrelation trace. Dots: experimental data, continuous line: sech^2 fit.

4. Discussion

Cascaded second-order mode-locking technique is found to be a proficient mechanism for the generation of stable ps pulse, never being affected by the Q-switching instability. That is probably due to the inverse saturation effect. To account for our CSM experimental results and optimize it appropriately, we need to calculate the nonlinear phase shift suffered by the FW beam after round trip through the NLC. The FW beam in its forward pass through NLC generates SH. If the phase difference $\Delta\vartheta = \vartheta_{2\omega} - 2\vartheta_{\omega}$, accumulated between the SH and FW beams due to propagation between the NLC and the OC, is properly adjusted, then the SH, in its backward journey through NLC, will continue to accumulate nonlinear phase to FW. We have solved these two cascaded processes theoretically using the coupled amplitude equations for two passes through NLC to calculate the total nonlinear phase shift $\Delta\vartheta$ at the end of the double pass. Our theoretical

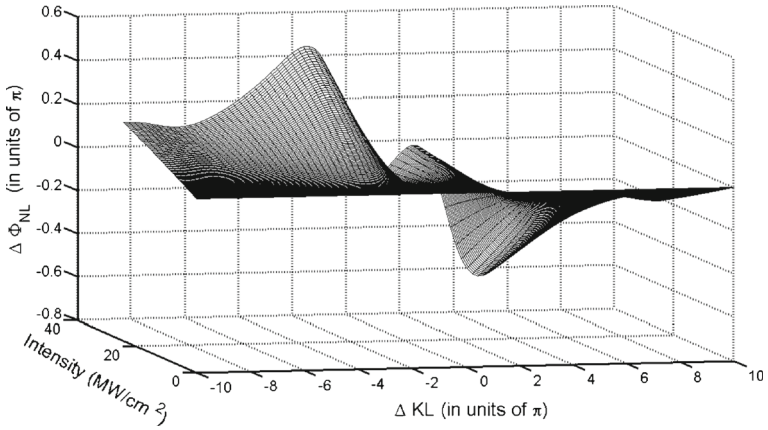

Figure 4. Nonlinear phase shift ($\Delta\Phi_{\mathrm{NL}}$) (in units of π), as a function of crystal phase mismatch, ΔkL (in units of π) and intracavity FW intensity at KTP crystal.

investigation shows that the complete back conversion of the SH beam into the FW takes place for $\Delta\vartheta = -\pi$, independent of the crystal phase mismatch. Figure 4 shows a plot of the nonlinear phase shift $\Delta\Phi_{\mathrm{NL}}$ (in units of π), as a function of intensity and phase mismatch, ΔkL (in units of π) on KTP crystal ($L = 9$ mm). The simulation shows that the phase shift changes sign at the phase-matching angle for all NLCs. Thus, the cascaded interaction gives rise to a self-focussing or defocussing similar to that of a Kerr medium, with an intensity-dependent refractive index given by $n = n_{\mathrm{FW}} + n_2^{\mathrm{eff}} I$, where I is the intracavity fundamental intensity at NLC. For large nonlinear phase shift, when $\Delta\Phi_{\mathrm{NL}}$ varies linearly with the intensity [3], n_2^{eff} can be calculated from (assuming nonlinear phase shift of $\Delta\Phi_{\mathrm{NL}}/2$ per pass) $\frac{\Delta\Phi_{\mathrm{NL}}}{2} = \frac{\omega}{c} n_2^{\mathrm{eff}} LI$. It is clear that for $\Delta kL < 0$, the nonlinear phase shift is positive and the NLC behaves as a self-focussing medium with positive n_2^{eff} and on the other side for $\Delta kL > 0$, we have a negative phase shift giving rise to a self-defocussing behaviour with negative n_2^{eff}. Our closed form Gaussian beam analysis of a resonator with an intracavity Kerr medium infers that the mode size at the laser gain medium decreases with increase of peak power when the cascaded nonlinear process makes the NLC to behave as a self-focussing medium corresponding to a positive nonlinear phase shift. From figure 4, it is clear that for $\Delta kL = -\pi$ both the nonlinear phase shift and the self-focussing power of the KTP reach a maximum, which gives maximum mode size variation at the laser gain medium. $\Delta kL = -\pi$ is obtained in the KTP crystal for an angle $\varphi = 25°5'38''$, the driving force for the CSM. As expected, we obtained a highly stable (independent of the controlling of the cavity elements), self-starting and self-sustained mode-locking for this optimum value of ΔkL. Inverse loss saturation saves the mode-locking from Q-switching instability at the cost of pulse broadening [10,11]. The group velocity mismatch (GVM) between the FW and the SH in the NLC broaden the pulse width as well [12]. This may be the reason for not getting the bandwidth-limited pulse width in CSM.

5. Conclusion

Second-order cascaded nonlinear interaction in an intracavity non-phase-matched second harmonic generation and down-conversion process produces large nonlinear phase shift on the FW wave and induces large $\mathrm{Re}(\chi_{\mathrm{eff}}^{(3)})$ to make nonlinear crystal to behave as a Kerr medium. After a comparative study on the performance of CSM for different nonlinear crystal and OC combinations, KTP with OC-3 is found to be the best candidate for CSM. When the KTP is placed at an angle $\varphi = 25°5'38''$, corresponding to a phase mismatch angle of 1.5°, it provides a positive $\Delta\Phi_{\mathrm{NL}}$, and KTP exhibits self-focussing behaviour. Closed form Gaussian beam analysis shows the cavity mode at the gain medium to decrease with the power for a self-focussing nonlinear crystal placed close to the OC. It gives direct nonlinear loss modulation through better overlapping between the pump and the cavity mode, resulting in an efficient and stable CSM. The soft aperture CSM laser developed generates dual colour picosecond pulses of 10.3 ps width at 1064 nm and 532 nm simultaneously from a single resonator. For an input pump power of 12 W, the laser delivers an average power of 1.84 W and 255 mW at 1064 nm and 532 nm respectively corresponding to a pulse repetition rate of 178 MHz at the optimum condition.

References

[1] D E Spence, P N Kean and W Sibbett, *Opt. Lett.* **16**, 42 (1991)
[2] M Piche and F Salin, *Opt. Lett.* **18**, 1041 (1993)
[3] R DeSalvo, D J Hagan, M Sheik-Bahae, G Stegeman and E W Van Stryland, *Opt. Lett.* **17**, 28 (1992)
[4] G I Stegeman, M Sheik-Bahae, E Van Stryland and Gaetano Assanto, *Opt. Lett.* **18**, 13 (1993)
[5] G Cerullo, S De Silvestri, A Monguzzi, D Segala and V Magni, *Opt. Lett.* **20**, 746 (1995)
[6] A Ray, S K Das, S Mukhopadhyay and P K Datta, *Appl. Phys. Lett.* **89**, 221119 (2006)
[7] S Mukhopadhyay, S Mondal, S P Singh, A Date, K Hussain and P K Datta, *Opt. Express* **21**, 454 (2013)
[8] K A Stankov and J Jethwa, *Opt. Commun.* **66**, 41 (1988)
[9] P K Datta, S Mukhopadhyay, S K Das, L Tartara, A Agnesi and V Degiorgio, *Opt. Exp.* **12**, 4041 (2004)
[10] P K Datta, S Mukhopadhyay, G K Samanta, S K Das and A Agnesi, *Appl. Phys. Lett.* **86**, 151105 (2005)
[11] T R Schibili, E R Thoen, F X Kartner and E P Ippen, *Appl. Phys. B* **70**, S41 (2000)
[12] M Zavelani-Rossi, G Cerullo and V Magni, *IEEE J. Quantum. Electron.* **34**, 61 (1998)